

# Synthesis of nanosized zinc ferrites from liquid precursors in RF thermal plasma reactor

Ilona Mohai<sup>a,\*</sup>, Loránd Gál<sup>a</sup>, János Szépvölgyi<sup>a,c</sup>, Jenő Gubicza<sup>b</sup>, Zsuzsa Farkas<sup>c</sup>

<sup>a</sup> *Institute of Materials and Environmental Chemistry, Chemical Research Center, Hungarian Academy of Sciences, H-1525 Budapest, POB 17, Hungary*

<sup>b</sup> *Department of Solid State Physics, Eötvös University, H-1518 Budapest, POB 32, Hungary*

<sup>c</sup> *Pannon University, H-8200 Veszprém, Egyetem u. 2, Hungary*

Available online 6 June 2006

## Abstract

Micro- and nanosized zinc ferrite particles were prepared in RF thermal plasma conditions. Ethanol solutions of the mixture of zinc- and iron-nitrates were used as precursors. In the experiments, effects of synthesis conditions on the properties of products were investigated. The products were characterized for chemical and phase composition, morphology and magnetic properties. Zinc ferrite particles having ferrimagnetic properties were produced which refers to formation of zinc ferrites of inverse spinel structure in particular conditions.

© 2006 Elsevier Ltd. All rights reserved.

**Keywords:** X-ray methods; Magnetic properties; Ferrites; Spinel; RF thermal plasma

## 1. Introduction

Spinel ferrites are widely used in different industries, e.g. as adsorbents,<sup>1</sup> as catalysts,<sup>2</sup> pigments<sup>3</sup> and materials of devices for electronic and magnetic storage of information. Applications require nanosized ferrites in many cases. Thus, synthesis and studies on the properties of zinc ferrites is an interesting research topics now.

Ferrite spinels crystallize in face centered cubic lattice. In the normal zinc ferrite structure, Zn<sup>2+</sup> ions are in tetrahedral, while Fe<sup>3+</sup> ions are in octahedral positions. Zinc ferrites having normal spinel structure exhibit paramagnetic properties at room temperature.<sup>4</sup> Under extreme conditions, such as mechanochemical activation,<sup>5</sup> rapid quenching<sup>6</sup> or coprecipitation followed by annealing<sup>7</sup> position of Zn<sup>2+</sup> and Fe<sup>3+</sup> cations in the crystal structure can be partially or even completely reversed. The strong super-exchange interaction among these sites results in an unusually high magnetization as compared to normal spinels.<sup>6</sup>

Thermal plasmas, such as direct current (dc) arcs<sup>8</sup> and radiofrequency<sup>9,10</sup> (RF) plasmas offer unique advantages for the synthesis of special ceramic powders due to the easily achievable high temperatures and energy densities. In an RF thermal plasma

flame the gas temperatures may exceed 10<sup>4</sup> K independently of the gas composition. In addition, a high temperature gradient exists between the hot plasma flame and the surrounding gas phase. The resulting rapid quenching rate is favourable for producing fine particles with unstable structures in thermodynamic terms.

In this paper results on the RF thermal plasma synthesis of zinc ferrites from the ethanol solutions of the corresponding nitrates are presented. Aim of the study was to find correlations between plasma parameters and properties of product.

## 2. Experimental

The experiments were performed in a radiofrequency thermal plasma reactor operating at a maximum plate power of 30 kW. The experimental set-up is shown in Fig. 1. Argon was used as plasma gas with a flow rate of 20 l min<sup>-1</sup>. The sheath gas was a mixture of Ar and O<sub>2</sub> with flow rate of 23 and 20 l min<sup>-1</sup>, respectively.

The precursor solutions were prepared by the dissolution of analytical grade Fe(NO<sub>3</sub>)<sub>3</sub>·9H<sub>2</sub>O and Zn(NO<sub>3</sub>)<sub>2</sub>·6H<sub>2</sub>O powders in technical grade ethanol using a magnetic stirrer. The Fe to Zn molar ratio was set to 2:1 in all cases.

The ethanol solutions of corresponding nitrate salts were injected into the plasma flame by a TEKNA suspension feeder. The solutions were atomized by argon with flow rate of

\* Corresponding author. Tel.: +36 1 438 1130; fax: +36 1 438 1147.  
E-mail address: [mohaiti@chemres.hu](mailto:mohaiti@chemres.hu) (I. Mohai).

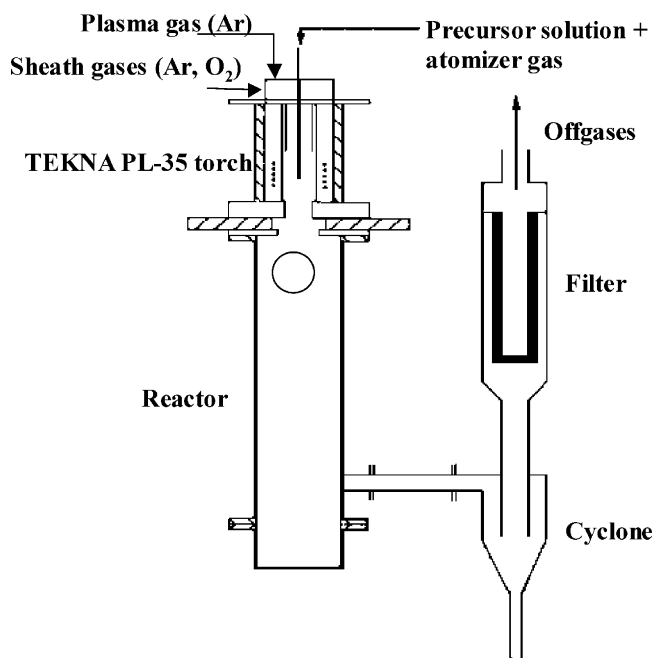


Fig. 1. Experimental set-up.

31 min<sup>-1</sup>. Inlet of injection probe was positioned at distances of 83 and 103 mm, respectively, below the top of induction coil. In the tests the following parameters were varied:

- Plate power.
- Concentration of salts in the ethanol solution.
- Position of injection probe.

The experimental conditions are summarized in Table 1.

The reaction products were collected from the reactor wall. Their chemical composition was analyzed by ICP-OES (Thermo Jarrell Ash Atomscan 25). A Philips Xpert XRD apparatus operating with Cu K $\alpha$  radiation was used to analyze the phase composition. The lattice parameters ( $a$ ) of the crystalline phases were determined from the positions of relevant diffraction peaks. Composition of zinc ferrite phase was determined from the lattice parameters. Morphology of products was studied by SEM (Philips XL30 ESEM) and TEM (Philips CM20). Energy dispersive X-ray fluorescence spectroscopy (EDS; NORAN EDS system) was applied to analyze the Fe and Zn content of indi-

Table 2  
Results of the plasma tests

Run	Zinc ferrite (ZnFe <sub>2</sub> O <sub>4</sub> )		Magnetite (FeFe <sub>2</sub> O <sub>4</sub> )	Saturation magnetization (emu g <sup>-1</sup> )
	$a$ (Å)	$I_{rel}$ (%)	$I_{rel}$ (%)	
1	8.440	100	54	25
2	8.441	100	57	26
3	8.441	100	13	20
4	8.440	100	84	28
5	8.438	100	35	20
6	8.438	100	31	28
7	8.438	100	51	32
8	8.438	100	23	16

$a$ : lattice parameter,  $I_{rel}$ : relative XRD intensities (731).

vidual particles. Magnetization measurements were performed at room temperature by a vibrating-sample (Foner-type) magnetometer. The external magnetic field varied up to 20,000 Oe. The saturation magnetization was determined by extrapolating the linear high-field part of the magnetization curve to zero fields.

### 3. Results and discussion

The experimental results are summarized in Table 2. For evaluation of experiments, the XRD intensity ratio of stoichiometric zinc ferrite (ZnFe<sub>2</sub>O<sub>4</sub>) related to magnetite (FeFe<sub>2</sub>O<sub>4</sub>) and the morphology of products were chosen. Composition of the spinel structure was determined by deconvoluting the 731 spinel reflection of X-ray diffractograms.

Products from the different runs had the same bulk Fe/Zn molar ratio as the precursor solutions (Fe/Zn = 2). Plasma treatment of precursors resulted in extensive spinel formation in all experiments (Fig. 2). Mainly spinels of zinc ferrite type were formed. However, formation of magnetite (FeFe<sub>2</sub>O<sub>4</sub>) was detected, as well. Intensity of the magnetite reflection related to that of zinc ferrite varied in a broad range (13–84%) with the experimental parameters (Table 2). Low magnetite content of the spinel phase was measured in processing of more concentrated solution at high plate power (Run 3) and also in processing less concentrated solutions at low plate power (Run 8). In both runs the injection probe was situated at the higher position (83 mm). Lowering the probe position by 20 mm resulted in the slight increase of the magnetite content (Runs 5 and 6). Highest

Table 1  
Experimental conditions

Run no.	Probe position (mm)	Plate power (kW)	Zn + Fe molar concentration (mol/l)	Feed rate (l/min)	Specific energy (kWh/mol Zn + Fe)
8	83	15	1.95	0.018	7.1
2	83	15	3.9	0.014	4.6
4	83	25	1.95	0.021	10.2
3	83	25	3.9	0.014	7.6
6	103	15	1.95	0.019	6.7
1	103	15	3.9	0.010	6.4
7	103	25	1.95	0.019	11.2
5	103	25	3.9	0.013	8.2

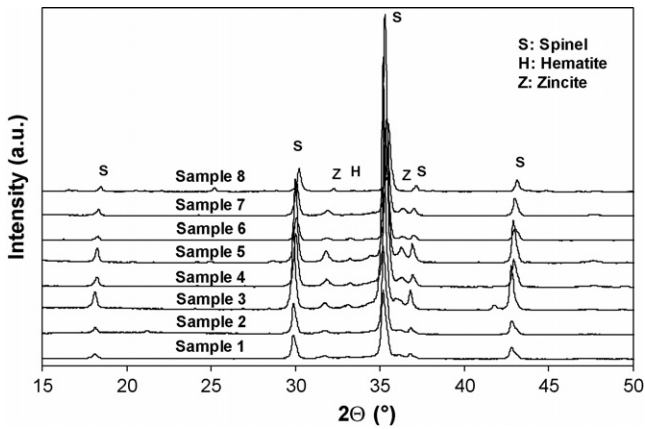


Fig. 2. X-ray diffractograms of products from Runs 1–8.

magnetite content was observed in Run 4, when the precursor endured the highest specific energy (10.2 kWh/mol). The specific energy ( $E_{sp}$ ) was defined as the plate power related to the feed rate of precursors.

Plotting of relative intensities of magnetite against the specific energy exhibits minimum type correlations for both settings of the injection probe (Fig. 3). At probe position of 83 mm the effect of specific energy is more pronounced than at 103 mm. In the former case, the precursor solution was injected to a zone where gas temperature and velocity was higher than at 103 mm probe position.

Run of curves in Fig. 3 is explained as follows. Thermodynamic calculations using Fachtstage<sup>®</sup> code revealed that in equilibrium conditions in the Zn–Fe–O system, in the temperature range of 500–1500 °C, the only stable condensed phase is ZnFe<sub>2</sub>O<sub>4</sub>. At 1750 °C both liquid magnetite and solid ZnO may exist. At temperatures above 1750 °C the total zinc content of the system is to be found in vapor phase. The liquid magnetite forms a stable phase up to 2250 °C. Above this temperature the liquid iron oxide gradually loses its oxygen content forming liquid FeO. At 3000 °C all components in the Zn–Fe–O system are vaporized.

Spraying the ethanol solution of the precursors into the hot plasma, in the first step solid particles are formed by the evaporation of the solvent from the spray drops, preserving their original size. In the dried drops nitrate salts decomposed and produced the mixture of the corresponding oxides.

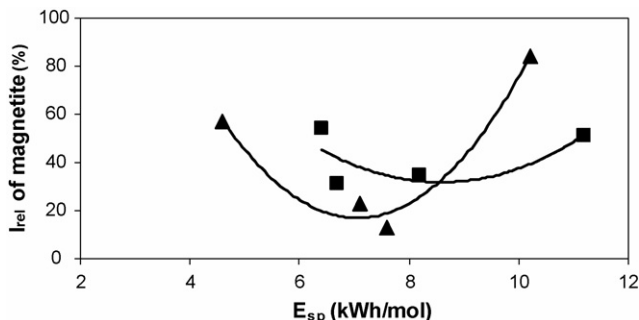


Fig. 3. Relative intensity of the magnetite reflection as plotted against specific energy. (▲) Probe position: 83 mm and (■) probe position: 103 mm.

At low specific energies (4–6 kWh/mol) the energy input is too low for the complete evaporation of zinc and iron oxides formed during thermal decomposition of nitrate precursors. However, the solid state reactions resulting in ZnFe<sub>2</sub>O<sub>4</sub> can proceed due to the intimate mixing of oxides. Surface temperature of the oxide grains in the hot plasma can be as high as 1500–2000 °C which is high enough to sublimate of ZnO and to result a spinel structure with higher Fe/Zn molar ratio (Run 2).

At specific energies of 10–12 kWh/mol, when diluted solutions are fed at high plate power (Run 4), the spray droplets are most probably vaporized in a great extent. Thus, reactions leading to spinel formation take place in vapor phase. Products of particular reactions are cooling very rapidly downwards the plasma flame region due to the intensive heat transfer over there. The iron oxides start to condense at about 2750 °C. Thus, they cannot react with ZnO at high conversion. Solid ZnO starts to form below 2000 °C. Moreover, voluminous plasma (Ar), auxiliary (O<sub>2</sub>) and reaction (CO<sub>2</sub>, H<sub>2</sub>O) gases contain condensed oxide particles in low concentration which further limits the solid state reaction between them.

At optimum conditions ( $E_{sp}$  = 6.7–8.2 kWh/mol) the evaporation of spray droplets and the solid state reactions of particles take place simultaneously. Evaporation rate is high enough to

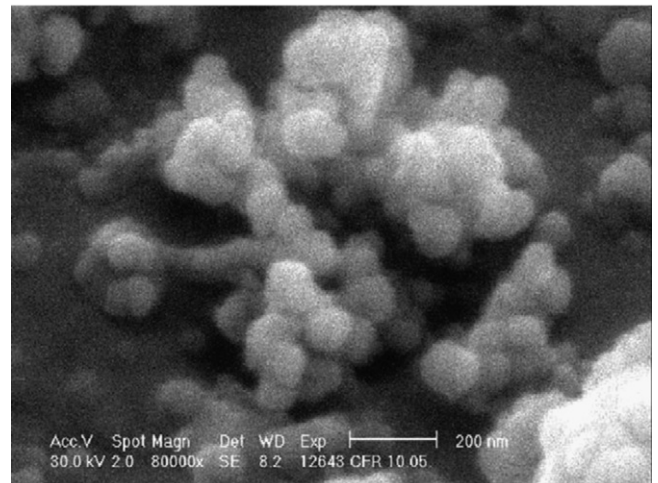
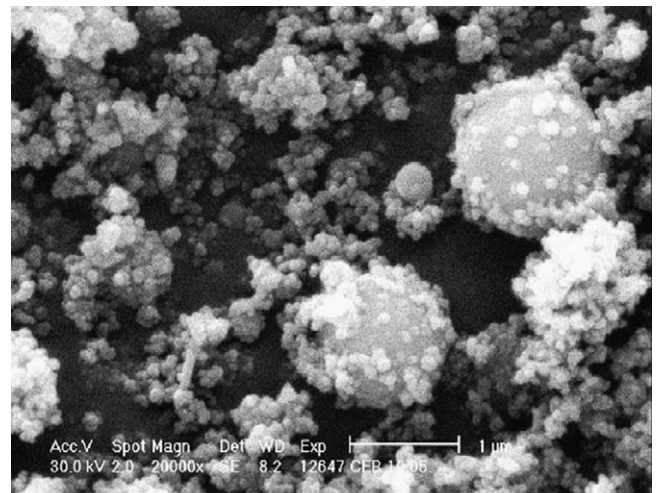


Fig. 4. SEM photos of product from Run 3.

ensure suitable concentration of species in the gas phase and the temperature and heat transfer conditions are suitable for effective solid phase reactions (Run 3).

Saturation magnetization of the products exhibited rather poor correlation with the  $ZnFe_2O_4/FeFe_2O_4$  intensity ratio. It suggests formation of inverse  $ZnFe_2O_4$  spinel structure with ferrimagnetic properties.

Investigation of the morphology of the products by scanning electron microscopy made clear that the spinels were formed by

two different mechanisms. All products contained microsized particles along with nanosized ones in various ratios. Depending on the size of the solid grains formed during decomposition of precursors and the plasma parameters, microsized or nanosized particles are formed. Parameters of Run 3 favoured the formation of nanoparticles by the complete evaporation of the solid grains followed by condensation and spinel formation. This sample contained only a few bigger spheres of  $\sim 1 \mu\text{m}$  size (Fig. 4). On the other hand, in the product of Run 7 most particles have sizes around  $20 \mu\text{m}$  (Fig. 5). Surface of microsized particles is covered by nanoparticles. In some dried drops, along with the

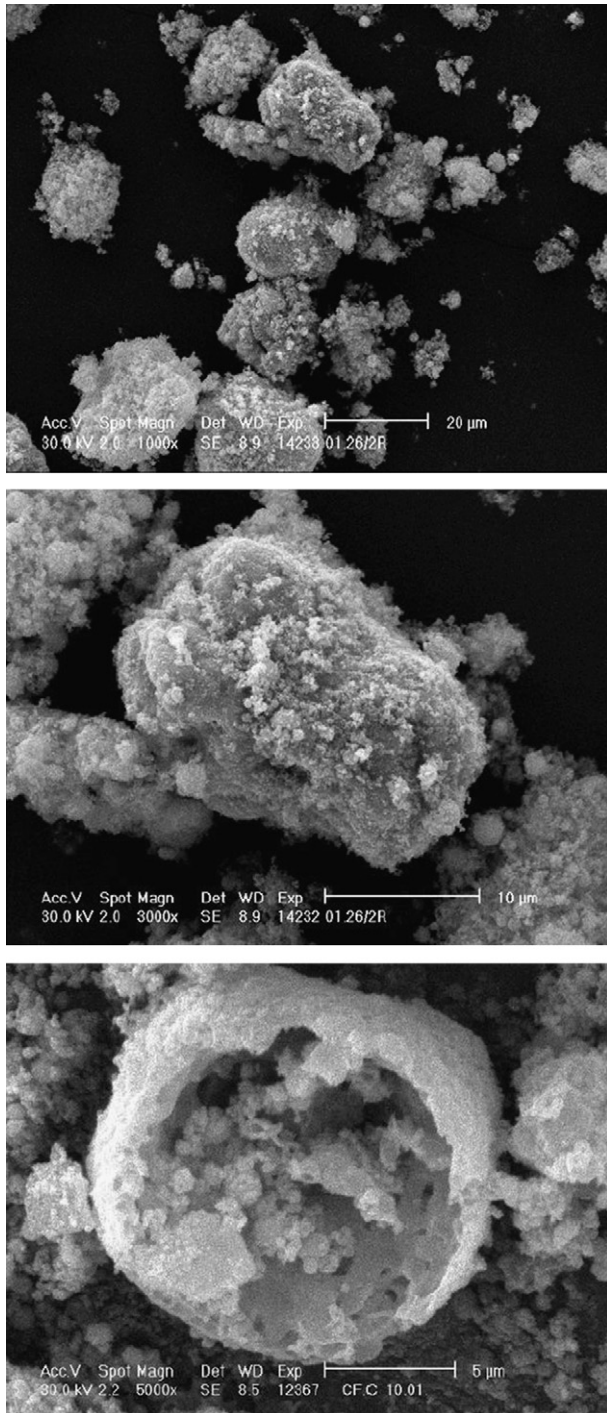


Fig. 5. SEM photos of product from Run 7.

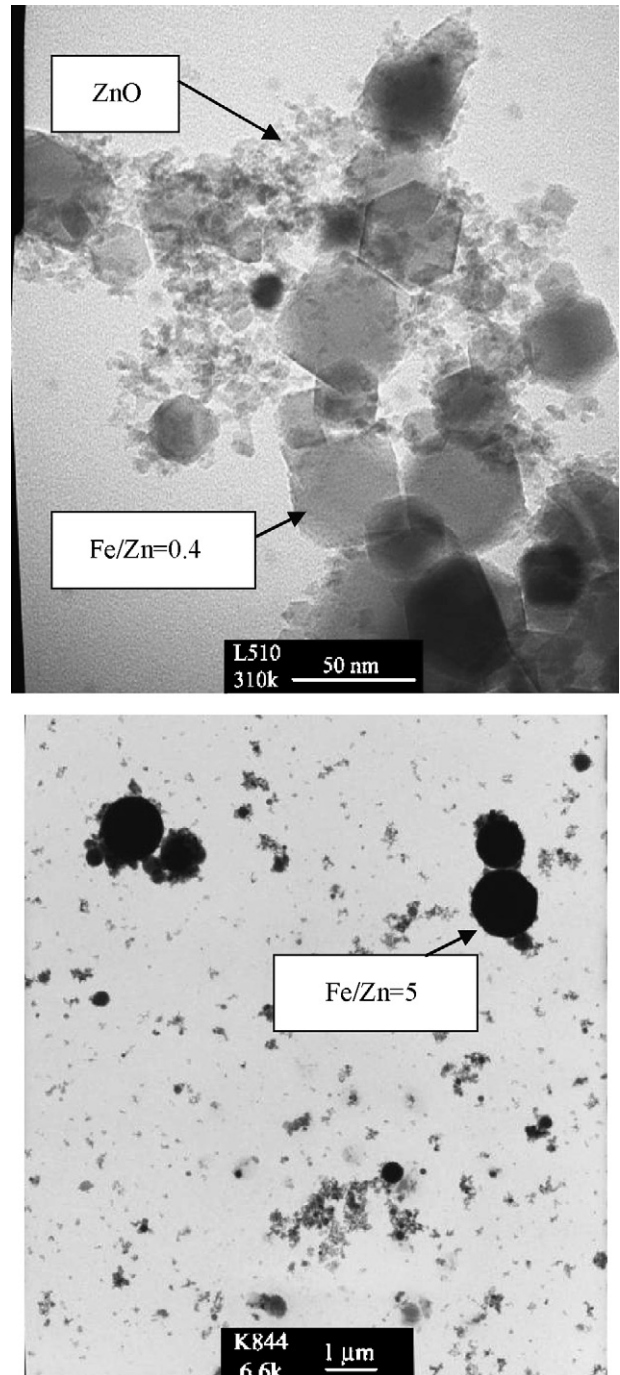


Fig. 6. TEM and EDS results of product from Run 1.

solid state reaction, partial evaporation of the oxides occurred as well. In the experimental conditions of Run 7 the spinels were mainly formed in solid state reactions.

In the TEM micrographs particles can be classified according to their size and chemical composition (Fig. 6). Chemical composition, represented by the Fe/Zn atomic ratio from EDS measurements varied with the size of the particles. The smallest (5 nm) particles proved to be pure ZnO. Increase of particle size was accompanied by a gradual increase of iron concentration. Crystals of 30–50 nm size had an average Fe/Zn ratio of 0.4/1. Composition of particles having the size about 100–300 nm is close to the stoichiometric Fe/Zn ratio of 2:1. In the micro-sized particles the Fe to Zn atomic ratio may be as high as 5:1.

#### 4. Conclusions

Radiofrequency thermal plasma treatment of the ethanol solution of zinc- and iron-nitrates resulted in an extensive spinel formation. The main reaction product was ZnFe<sub>2</sub>O<sub>4</sub>. However, depending on the reaction conditions, different amounts of magnetite (FeFe<sub>2</sub>O<sub>4</sub>) were formed, as well. Saturation magnetization exhibited rather poor correlation with the FeFe<sub>2</sub>O<sub>4</sub>/ZnFe<sub>2</sub>O<sub>4</sub> intensity ratio. It suggests formation of inverse ZnFe<sub>2</sub>O<sub>4</sub> spinel with ferrimagnetic properties. Morphology of the products had a strong dependence on the synthesis conditions. Particle size is hardly influenced by the size of spray droplets fed into the hot plasma flame. Due to the short residence time in the hot zone, the bigger (10–20 μm) droplets cannot evaporate completely. In these grains the spinel structure is formed in solid state reactions between oxides. As ZnO is susceptible to sublimate at high temperature, in these cases Fe/Zn atomic ratio is higher than the stoichiometric ratio. Thus, ZnO is concentrated in the nanosized grains. For the RF plasma synthesis of ferrite spinels of well-defined bulk composition, use of ethanol solutions of

the corresponding metal salts as precursors is recommended. However, synthesis conditions, including plasma parameters and nebulization efficiency should be carefully tested and controlled.

#### Acknowledgements

This work was supported by the grants of OTKA Nos. T047360 and F047057 and GVOP-3.1.1-2004-05-0031/3.0.

#### References

1. Ahmed, M., Alonso, L., Palacios, J. M., Cilleruelo, C. and Abanades, J. C., Structural changes in zinc ferrites as regenerable sorbents for hot coal gas desulfurization. *Solid State Ionics*, 2000, **138**, 51–62.
2. Yürüm, Y., ed., *Clean Utilization of Coal: Coal Structure and Reactivity, Cleaning and Environmental Aspects, NATO ASI Series 370*. Kluwer, 1992, pp. 221–237.
3. Schiessl, W., Potzel, W., Karzel, H., Steiner, M., Klavius, G. M. et al., Magnetic properties of the ZnFe<sub>2</sub>O<sub>4</sub> spinel. *Phys. Rev. B*, 1996, **53**, 9143–9152.
4. Cullity, B. D., *Introduction to Magnetic Materials*. Addison-Wesley, Reading, MA, 1972, pp. 181–190.
5. Druska, P., Steinike, U. and Sepelak, V., Surface structure of mechanically activated and of mechano-synthesized zinc ferrite. *J. Solid State Chem.*, 1999, **146**, 13–21.
6. Tanaka, K., Makita, M., Hirao, K. and Soga, N., Effect of heat treatment on magnetic properties of ferrimagnetic zinc ferrite prepared by rapidly quenching method. *J. Magn. Soc. Jpn.*, 1998, **22**(S1), 77–79.
7. Jeyadevan, B., Toji, K. and Nakatsuka, K., Structure analysis of coprecipitated ZnFe<sub>2</sub>O<sub>4</sub> by extended X-ray absorption fine structure. *J. Appl. Phys.*, 1994, **76**, 6325–6327.
8. Fukumasa, O. and Fujiwara, T., Rapid synthesis of ferrite particles from powder mixtures using thermal plasma processing. *Thin Solid Films*, 2003, **435**, 33–38.
9. Mohai, I., Szépvölgyi, J., Bertóti, I., Mohai, M., Gubicza, J. and Ungár, T., Thermal plasma synthesis of zinc ferrite nanopowders. *Solid State Ionics*, 2001, **141/142**, 163–168.
10. Mohai, I. and Szépvölgyi, J., Treatment of particulate metallurgical wastes in thermal plasmas. *Chem. Eng. Process.*, 2005, **44**, 225–229.